Navigator Echoes

BioE – 594 Advanced Topics in MRI

Mauli. M. Modi.

What are Navigator Echoes?

- In order to ***correct the motional artifacts*** in Diffusion –weighted MR images, a modified pulse sequence is proposed which uses the phase information from ***an additional spin echo*** to correct for patient motion.
- These echoes are ***Navigator Echoes.***
- Post processing of the navigator echo data provides a highly detailed ***record*** of the ***displacements*** and ***phase shifts*** that occur during imaging.

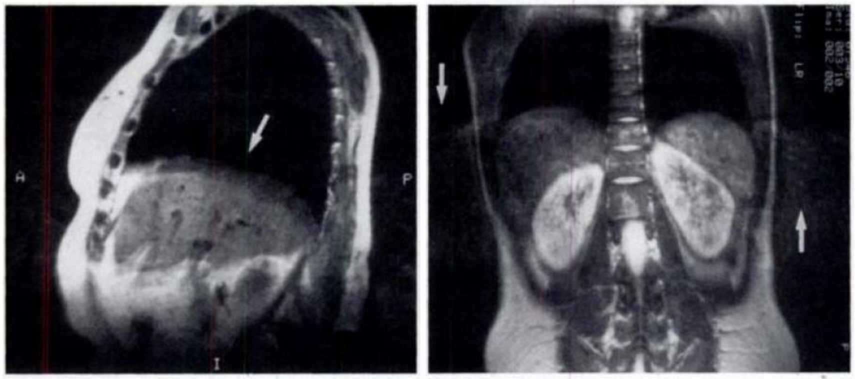

a. b.

Figure 1. Effects of respiratory motion. **(a)** Sagittal, short TR/TE image of the thorax and abdomen. Anteroposterior motion of the anterior body wall causes subtle arclike artifacts that are superimposed on the abdominal contents. Much more important is the unsharpness caused by the craniocaudal respiratory motion of the diaphragm and abdominal organs. This is apparent as blurring of the dome of the diaphragm (arrow) and a doubled appearance at the inferior margin of the liver. These effects are due to temporal modulation of the modulus of the transverse magnetization as tissues move from voxel to voxel. **(b)** Coronal T2-weighted image of a different patient. Respiratory craniocaudal motion of the liver and spleen causes displaced ghost images of these organs, which are apparent on both sides of the abdomen (arrows). These effects are due to temporal modulation of the phase of the transverse magnetization of volume elements.

Why Navigator Echoes??

- Phantom studies demonstrated that the technique can ***directly correct image degradation*** caused by motion.
- In contrast to conventional artifact reduction techniques such as ordered phase encoding and gradient moment nulling, this new method has a unique capacity to ***reduce motion un-sharpness.***
- The technique can markedly improve images degraded by voluntary motion and shows promise for addressing the problem of respiratory motion in thoracoabdominal imaging.

Measurement of motion with NAV echoes.

- The task of measuring displacements and phase shifts becomes ***more challenging*** when combinations of ***mobile and static structures*** are present in the field of view.

History of Motion correction techniques.

- A variety of techniques for reducing motion degradation in MR images have been introduced in the past several years:

1. Physiologic gating.
2. Ordered phase encoding.
3. Gradient moment nulling.
4. Presaturation.

Navigator Echoes

- During MR acquisition, motion causes changes in the position of the structures in the field of view from one phase encoding measurement to another. This is known as ***view-to-view changes***.
- During the process of measuring a single phase encoding view, moving tissue and flowing blood can cause variable phase shifts. We call these as ***intraview effects***.

Measurement of view-to-view displacement.

- NAV echo is similar to an image echo, except that ***no phase encoding*** is applied.
- This implies that the NAV echo data will vary from view to view ***only if motion along the x-axis is present***.
- The order of the echoes could be reversed if desired.
- In that case phase encoding would be applied before the first (image) echo and then would be ***unwound*** by an additional y-axis gradient before the NAV echo.

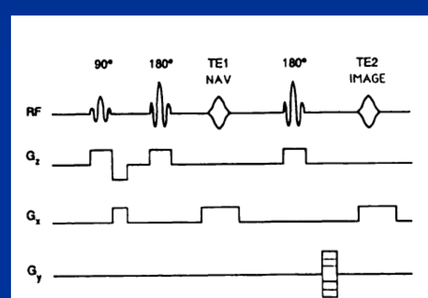

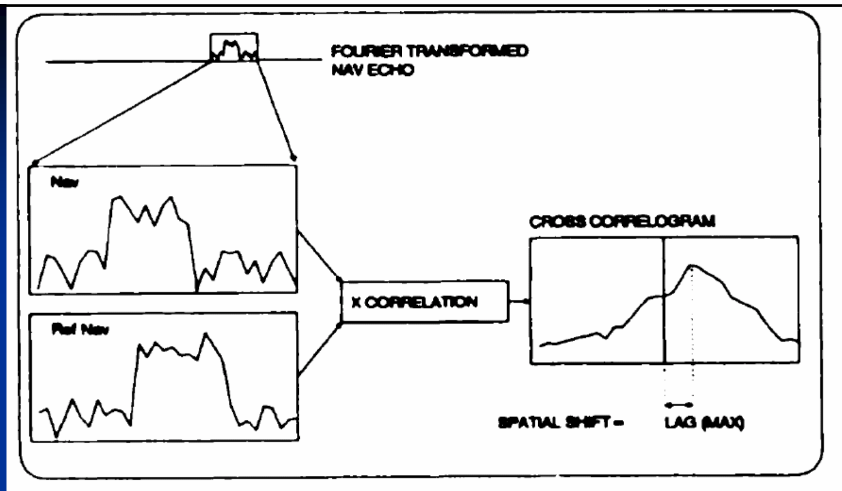

- Processing of successive NAV echoes is done in such a way that the ***x-axis displacements*** of a moving object can be ***determined*** with respect to a ***reference view***.
- The X-NAV echoes are ***Fourier transformed*** into projections in the hybrid space and modulus values are calculated.
- A ***single NAV projection*** is arbitrarily chosen as a ***reference*** and cross-correlation functions are calculated with respect to each of the other NAV projections.

- The value corresponding to the maximum value in each cross-correlation function is then a measure of the x displacement of the object w.r.t. the reference NAV view.
- We have assumed that the motion is not so rapid that a significant displacement would occur in a short time (10-20ms) bet the NAV and image echoes.

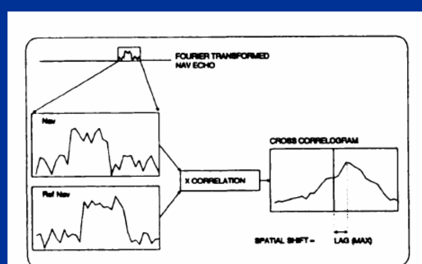

3.

- It may be desirable to use the first echo for imaging and the second for NAV information in sequences with short repetition times (TR’s) and echo times (TE’s).
- Other variants could use gradient echoes for NAV purposes rather than spin echoes and minimize cycle time or to avoid sacrificing an imaging echo.

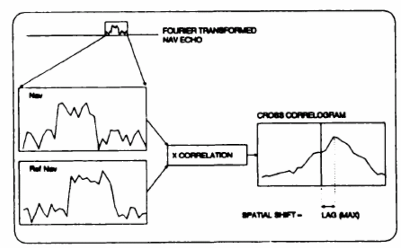

3.

- Displacement along the Y-axis could be similarly obtained by applying the read-out gradient of the NAV echo along the y axis rather than along x.
- A combined XY- NAV sequence could incorporate an X-NAV echo before the image echo and a Y-NAV echo after it.

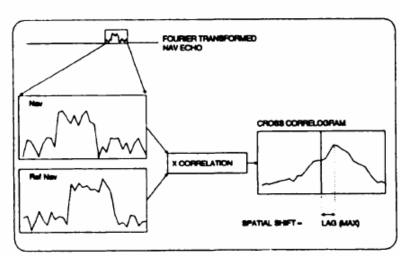

3.

Measurement of Phase shifts due to intra-view motion.

- Consider a X- NAV sequence.
- If intra-view motion causes a bulk phase shift, it will be detectable in the hybrid NAV data in the segment in which the modulus of the object is concentrated.
- The phase shift due to intra-view motion can be determined for each NAV echo by calculating the phase angle of complex data points at appropriate locations in each NAV projection in hybrid space and then subtracting corresponding phase angles from a NAV projection obtained when the object is static.

- The motion-induced phase shifts observed in each NAV echo are proportional to the phase shifts present in the corresponding image echoes.
- If the proportionality constant can be determined with calculation or calibration, then the image echo data can be adaptively corrected for intra-view motion .

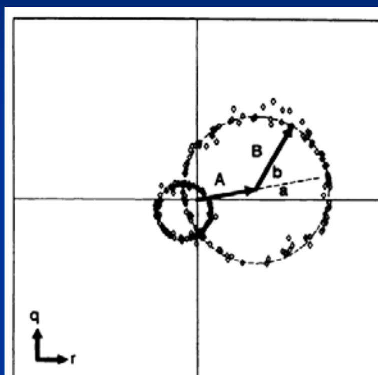

Figure B1. Phase shifts due to intraview motion (q = quadrature component of the spin echo, r = real component of the spin echo).

Algorithms for correction of Object Displacements and Motion-induced Phase shifts.

- A set of short intuitive derivation of a set of mathematical operations can correct MR imaging data for view-to-view displacements of an object in the x, y, and z directions
- We can also correct for phase shifts due to intra-view motion in any direction.

- The raw MR imaging data collected in a spin-warp acquisition can be ordered in an array with rows corresponding to individual phase-encoded spin echoes.
- This array can be regarded as a map of spatial frequencies and we will refer to this plane as ***data-space***.
- Each of the rows in the data array are Fourier transformed to yield a final complex image array.
- The intermediate array has spatial coordinates in the x-direction and spatial frequency coordinates in the y direction so that this plane is called the ***Hybrid space***.

Considerations

- Have separated the effects of displacement and phase shift in the discussion.
- For simplicity, we will focus on the case of a single moving object within the field of view.

View-to-view displacements in the x (frequency encoding) direction.

- Consider a single small object moves from position (x, y) to position (x- ▲x, y) in the time between acquisition of two spin echo signals.
- If both spin echoes were acquired with the same phase encoding, then the only difference between them is due to the displacement in the frequency-encoding direction.

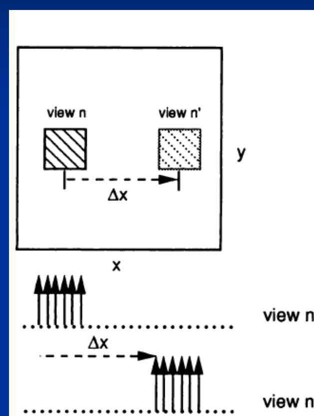

Figure A1. Displacement in the x direction.

- The difference is best appreciated by examining these data after they have been Fourier transformed :

$$\vec{S}_{jk}(\textit{data space}) \rightarrow \vec{S}_{xk}(\textit{hybrid space}), \qquad \textbf{(A1)}$$

$$\vec{S}_{xk} = \frac{1}{256} \sum_{j=0}^{255} \vec{S}_{jk} e^{+\frac{i2\pi jx}{256}}, \qquad \textbf{(A2)}$$

Where,

J : index for 256 samples of a spin echo

X axis in the hybrid space corresponds directly to the x axis in the image space.

- The effect of an object displacement by - ▲x is to shift the I, Q values in the hybrid space by the distance - ▲x.
- This suggests, that a particular spin echo view can be corrected for a known arbitrary displacement simply by Fourier transforming the data, shifting the data by + ▲x , and then inverse Fourier transforming back into data space.

- The Fourier shift theorem provides a way to implement this correction directly in data space.
- It states that if $f(x)$ has a Fourier transform $F(j)$ then $f(x - \Delta x)$ has a Fourier transform :

$$e^{-i2\pi \Delta x j} F(j)$$

- This constitutes a phase rotation of each complex point in the sampled spin echo.

- When the use of discrete transforms is considered, the phase rotation in the jth sample caused by displacement of Δx pixels would be

$$\Delta\phi_x = \frac{2\pi \Delta x j}{N_x}, \; j = 0 \text{ to } N_x - 1, \quad \text{(A3)}$$

Where N_x : total number of samples of the spin echo signal.

- The maximum rotation would be reduced by using the centre of the sampled echo as the zero point and rotating earlier points negatively :

$$\Delta\phi_x = 2\pi\Delta x\left[j - \left(\frac{N_x - 1}{2}\right)\right]\frac{1}{N_x}.$$

- If the position is accurately known relative to some reference position, this equation provides a method for adaptively correcting each digitized spin echo.

- When a 2DFT reconstruction is provided on a corrected data set, the final image should appear as if it were static at the reference position.
- The phase rotation can be implemented with the following formulas:

$$I' = I\cos(\Delta\phi) - Q\sin(\Delta\phi),$$
$$Q' = I\sin(\Delta\phi) + Q\cos(\Delta\phi),$$

Where I, Q are the original values and I', Q' are the corrected values.

View-to-view displacements in y (phase-encoding) direction.

- Consider a single small object that moves a distance Δy along the y-axis in the time between 2 spin echoes with identical phase encoding.
- The modulus Mxy of complex numbers in raw data space, hybrid space or image space is defined as:

$$M_{xy} = \sqrt{I^2 + Q^2}$$

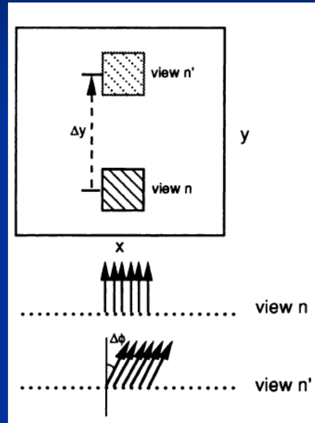

Figure A2. Displacement in the y direction.

- While there is no difference in the modulus of the two spin echoes in hybrid space, there is well defined phase difference due to application of phase encoding.
- The total phase twist in the y direction is given by:

$$\Delta\phi_y = 2\pi\left[k - \left(\frac{N_y - 1}{2}\right)\right].$$

- the phase difference caused by a displacement of Δy is given by:

$$\Delta\phi_y = 2\pi\Delta y\left[k - \left(\frac{N_y - 1}{2}\right)\right]\frac{1}{N_y}.$$

- To correct a spin echo for such y displacement it is simply necessary to rotate each I,Q vector in the hybrid space by the reverse of this phase angle.
- By the Fourier addition theorem this phase rotation can be applied to all of the points in the digitized spin echo in the data space.

View-to-view displacement in the z direction.

- In the case of section-selective 2-D Fourier transform imaging, it is not possible to adaptively correct raw data in retrospect for view-to-view displacements in the logical z direction.
- Such motions could be corrected if a 3D FT imaging process is used, as the z axis motion would be along either a frequency or phase encoding axis.

- On the assumption of the latter, the phase rotation for a 3D FT acquisition would be:

$$\Delta\phi_z = 2\pi\Delta z\left[l - \left(\frac{N_z - 1}{2}\right)\right]\frac{1}{N_z}$$

where,

Δz : pixel displacement along z

l : view number

N_z : total number of resolvable elements in that direction.

Bulk phase shifts due to intraview motion in the x, y, or z directions.

- Consider a single uniform object that moves at a given velocity during the time TE of a spin echo acquisition.
- We compare the spin echo signal obtained from this moving object to the signal that would be derived from a static object located at the same position at the time TE.
- The differences in the spin echo signals will be purely due to phase shifts of the transverse magnetization M_{xy}.

- The magnitude of the phase shift depends on:

1. The direction of motion with respect to the x,y and z axis.
2. The gradients applied in these directions.
3. The time derivatives of motion.

Combined corrections

- It is possible to combine all of the operations so that a data set can be adaptively corrected to reduce:

1. Artifacts
2. Intensity loss
3. Unsharpness due to view-to-view object displacements and intraview phase shifts.

Assumptions for combined corrections

- The correction is applied in data space, as the phase rotations associated with each correction can be summed together to yield a single corrective phase shift for each complex data point.

$$\vec{S}' = e^{-i\Delta\phi_c}\vec{S}, \qquad \text{(A12)}$$

where $\Delta\phi_c(j,k,l) = \Delta\phi_x + \Delta\phi_y + \Delta\phi_z + \Delta\phi_p$ (Eq 13) for three-dimensional Fourier transform and $\Delta\phi_c(j,k) = \Delta\phi_x + \Delta\phi_y + \Delta\phi_p$ (Eq 14) for two-dimensional Fourier transform.

Phantom Studies

- The NAV echo sequence illustrated in the fig was implemented on a 1.5 T imager.
- A variety of phantom studies where performed in the course of developing the adaptive correction technique.

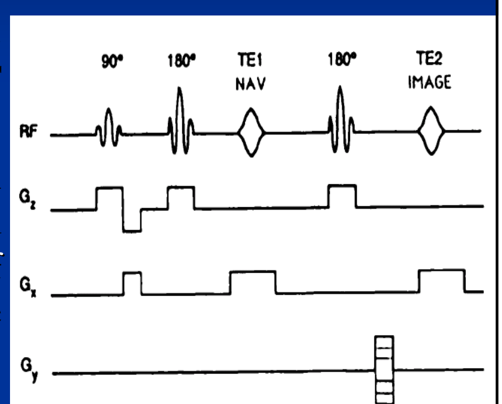

- A plastic bladder was filled with ultrasound gel to serve as a motion phantom.
- The irregular margins of the phantom and suspended air bubbles provided details for assessing the effectiveness of motion correction techniques.

- The phantom was imaged transversely while it was reciprocating at varying rates and amplitudes in the frequency-encoding direction during acquisition.
- The FOV was 24 cm and the section thickness 0.5 cm.

- All imaging was performed with 256 encoding views and 2 signal acquisitions.
- The TR and TE values are varied depending on the purpose of the experiment.
- The next figure shows the general scheme of data processing.

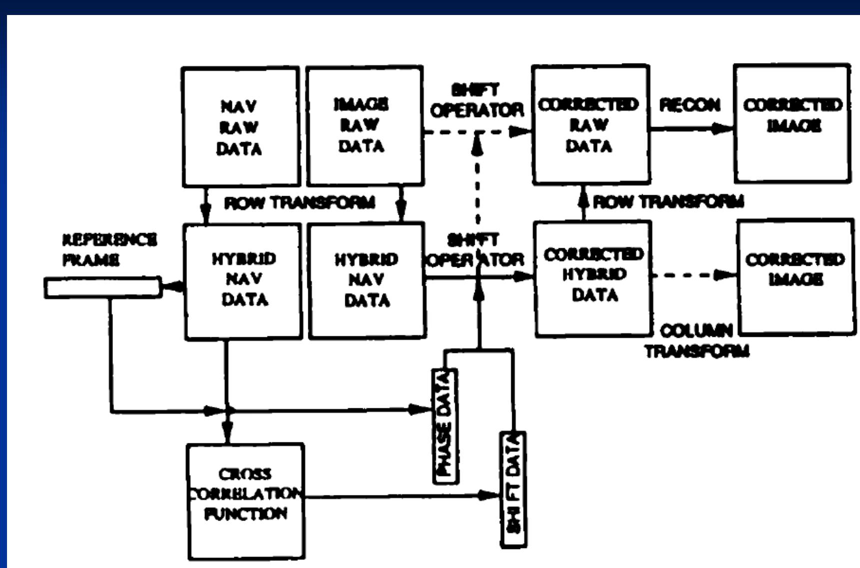

Results of Phantom Studies

- Provide a strong support for the adaptive correction concept.
- The fig shows an experiment to test the capacity of the adaptive correction method to correct data sets in which the motion effects are primarily due to view-to-view displacements.

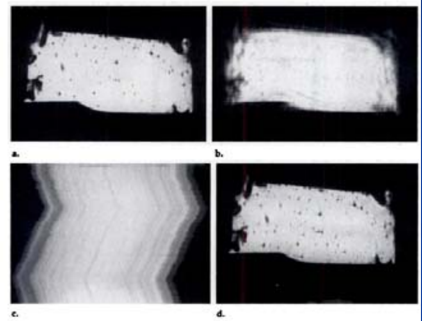

Figure 5. Adaptive correction of view-to-view displacement. **(a)** Image shows the appearance of the phantom in a motionless state. **(b)** Uncorrected image obtained with the X-NAV sequence when the phantom was manually moved from side to side (x direction) during acquisition at low velocities of less than approximately 1 cm/sec. Note the total loss of internal detail due to motion unsharpness and the presence of motion artifacts. **(c)** Image shows a portion of the X-NAV data obtained during the same acquisition. These echoes have been Fourier transformed, and their modulus is displayed in order of acquisition from top to bottom. Each horizontal raster line illustrates the transverse position of the phantom at the time the NAV echo was collected. **(d)** The X-NAV data were processed to determine the displacement of the phantom from a reference position at each time in the acquisition. With these data, the adaptive algorithm was applied to the same raw data used to make the image in b. The corrected raw data were reconstructed to yield the image in d. The correction technique has achieved the desired objective of correcting both artifacts and unsharpness.

- The phantom was shifted relatively slowly so that phase shifts due to intraview motion would be minimized.
- TR = 400 msec.
- NAV TE = 30 msec.
- Image TE = 70 msec.

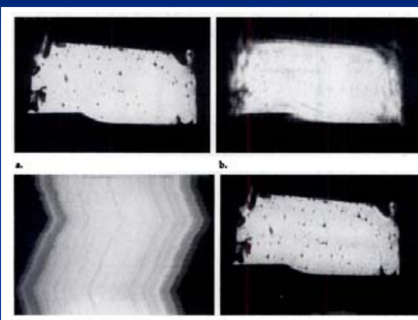

Figure 5. Adaptive correction of view-to-view displacement. **(a)** Image shows the appearance of the phantom in a motionless state. **(b)** Uncorrected image obtained with the X-NAV sequence when the phantom was manually moved from side to side (x direction) during acquisition at low velocities of less than approximately 1 cm/sec. Note the total loss of internal detail due to motion unsharpness and the presence of motion artifacts. **(c)** Image shows a portion of the X-NAV data obtained during the same acquisition. These echoes have been Fourier transformed, and their modulus is displayed in order of acquisition from top to bottom. Each horizontal raster line illustrates the transverse position of the phantom at the time the NAV echo was collected. **(d)** The X-NAV data were processed to determine the displacement of the phantom from a reference position at each time in the acquisition. With these data, the adaptive algorithm was applied to the same raw data used to make the image in b. The corrected raw data were reconstructed to yield the image in d. The correction technique has achieved the desired objective of correcting both artifacts and unsharpness.

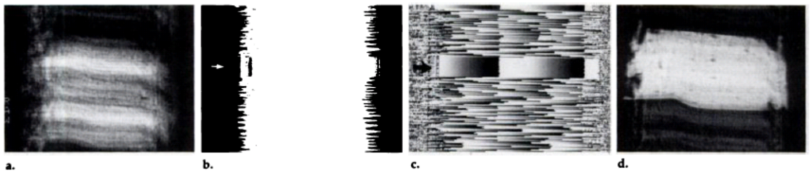

Figure 6. Combined displacement and phase shift correction. **(a)** Uncorrected image in which the phantom was shifted much more vigorously during acquisition. **(b)** Image shows the modulus of the transformed X-NAV echoes obtained during a portion of the acquisition. Note that although the rate of motion was generally high, there was a brief pause in the motion (arrow). **(c)** Image shows the phase of the same group of X-NAV projections. During the pause when the phantom was static (arrow), the phase of successive X-NAV projections was identical at corresponding x-axis locations from line to line. During vigorous motion, however, the phase along a vertical column of points varies from projection to projection. This is due to the effects of intraview motion. **(d)** The displacement and phase shift data extracted from the NAV echoes were used to correct the raw image data. These data were reconstructed to yield the image in **d,** which is substantially improved in comparison with the original in **a.** The residual artifact in **d** is largely due to aliasing of the phase shifts in the NAV data, a problem that can be corrected by adjusting the TE of the NAV echo.

- This illustrates an experiment in which the phantom was moved more rapidly (up to approx 5 cm/sec) thereby ***increasing the influence of intraview motion*** on the spin echo data.
- The influence of the intraview motion is well shown in the phase map of the NAV echoes. (Fig 6c)
- Fig 6d demonstrates the effectiveness of the technique when both methods are combined.

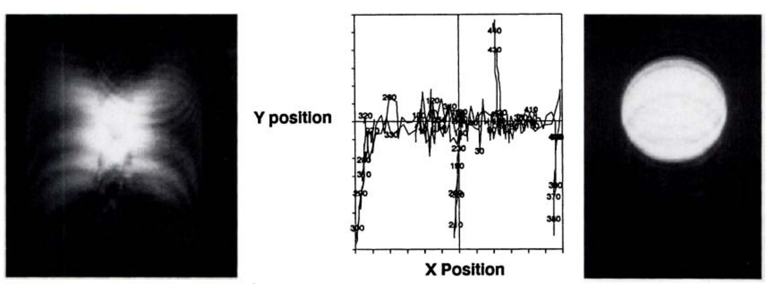

Figure 7. Two-dimensional displacement monitoring and correction. A cylindrical phantom filled with mineral oil was shifted slowly in the xy plane during image acquisition. The NAV echo sequence was modified to provide two-dimensional localization information from the single NAV echo. **(a)** Uncorrected image shows that the circular cross section of the phantom is completely lost due to motion. The NAV echo data were processed to extract the x and y coordinates of the object during image acquisition. The calculated trajectory of the object in the xy plane is shown schematically in **b.** The numbers along the course of the trajectory refer to the order of acquisition of NAV echoes, from 1 to 512. These data were used to correct for x and y displacements in the raw image data. **(c)** Reconstructed corrected image depicts the phantom much more clearly.

- This is a ***2D correction*** for both x and y displacements during imaging, with x and y displacement data ***derived from a single NAV echo***.
- Phase shifts due to intraview motion lead to error in the estimation of y position during imaging, factors causing residual artifacts in the corrected image.
- The corrected image is clearly improved as compared with the uncorrected image.

In vivo studies

- Preliminary in vivo studies were performed with the pulse sequence as illustrated in the figure.
- In the first in vivo experiments we evaluated the capacity of the technique to correct spontaneous voluntary motion of an extremity during image acquisition.

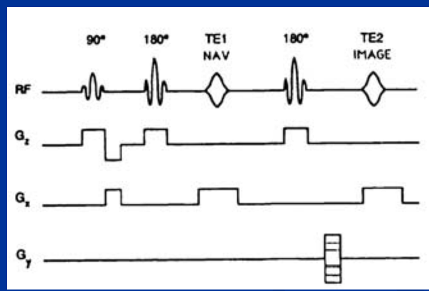

Example:

- a volunteer was asked to spontaneously shift one leg from side to side by approximately 2 cm during acquisition, while other extremity was fixed in place.
- The NAV echo sequence was used to image the abdomen of volunteers to assess the usefulness of this approach for measuring respiratory movements.
- Applied a correction for displacement to one of the studies.

Results of In Vivo studies

- This fig shows an example of one of the studies of the extremities.
- The NAV echo display clearly demonstrates the lateral movements during imaging.
- In processing the NAV data, it was necessary to exclude the segment of each NAV projection spanning the static leg.

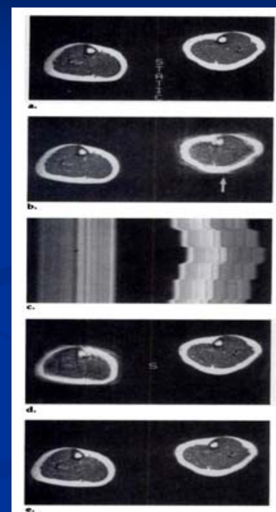

- The segment of exclusion can be identified by computing the variance of each column of the NAV data array.
- This also provides a template for selectively applying the correction to the image data in hybrid space to yield the regionally corrected image in fig e.

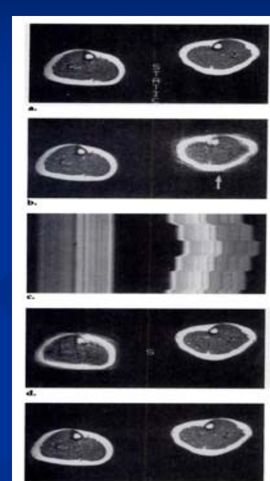

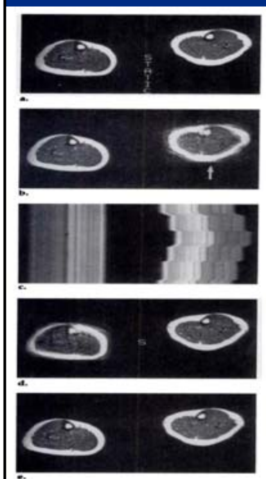

Figure 8. In vivo regional correction of voluntary motion. **(a)** Image shows a transverse section of the static legs of a volunteer. **(b)** A second acquisition shows that the left leg was moved spontaneously from side to side and the right leg was stationary. Note the artifacts and unsharpness caused by the leg motion (arrow). **(c)** Image shows the modulus X-NAV data obtained during the acquisition. The temporal pattern of motion of the left leg and the constant position of the right leg are clearly shown. **(d)** Image was obtained by applying a global adaptive correction to the raw data. X-displacement information for the left leg was provided by NAV echo data. The image of the left leg has been markedly improved and is almost equal to the static image. As expected, the image of the right leg is now degraded by "pseudomotion" imparted by the correction process. **(e)** Image was obtained by using a regional correction. The effects of the motion of the left leg are eliminated while the right leg is still depicted clearly.

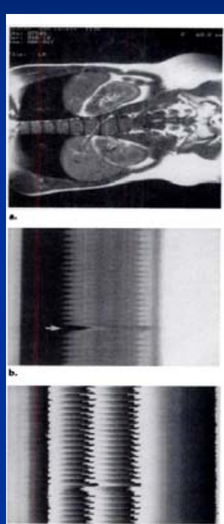

Figure 9. In vivo tracking of diaphragm motion with NAV echoes. **(a)** Uncorrected coronal spin-echo image of the abdomen, obtained with a TR of 500 msec, shows the right and left hemidiaphragm, liver, spleen, and kidneys. The frequency-encoding (x) axis is oriented longitudinally in this acquisition. **(b)** Image shows the modulus of transformed X-NAV echoes. Note the wave-like pattern at interface between the low intensity of the thorax and the higher intensity of the abdomen, which reflects the craniocaudal motion of normal, quiet tidal breathing (excursions of approximately 2.5 cm in this subject). The larger diaphragm movement (arrow) of approximately 6 cm is a sighing respiration that periodically appears in normal, quiet breathing patterns. **(c)** Phase display of the transformed X-NAV echoes shows the cyclical phase shifts caused by intraview motion and the slightly larger and more prolonged phase disturbance caused by the sighing respiration. This example provides evidence for the feasibility of measuring respiratory movements simultaneously with image acquisition.

- The ability of NAV to track visceral motion is shown in the figure.

a. b.

Figure 10. Adaptive correction of respiratory motion. **(a)** Uncorrected coronal image (TR of 400 msec, TE of 40 msec) of the abdomen of a volunteer, obtained with 256 views, two signal averages, and a section thickness of 5 mm. Sequence included a NAV echo with a TE of 20 msec. The unsharpness of the diaphragm caused by craniocaudal respiratory motion is readily appreciated (arrowheads). Similar unsharpness is apparent at the upper and lower poles of the kidneys and in the poor definition of the fat plane between the liver and the right kidney (arrow). **(b)** Information from the NAV echo data has been used to correct the data for view-to-view displacements in the craniocaudal direction. Note that the contour of the diaphragm (white arrowheads) is much sharper in this image than in the uncorrected image. Similarly, the upper and lower poles of the kidneys are more clearly defined, and the fat plane between the liver and right kidney is much sharper (black arrow). Most important, intrahepatic vascular structures (white arrow) and the right adrenal gland (black arrowhead) are visible in the corrected image, whereas they were essentially invisible without the adaptive correction technique.

- A correction for view-to-view displacements was applied to a coronal image of the abdomen obtained with the NAV echo sequence.
- The most important observation is that the corrected image depicts structures that are not evident at all in the conventional stage.

Discussion

- Results demonstrate that the adaptive correction technique is capable of directly addressing many of the effects of motion in MR images.
- Compared to other techniques, which only reduce the artifacts, this method has a ***unique capability to reduce motion unsharpness.***
- There are ***few practical penalties*** associated with the use of NAV sequence.

- On the basis of the implementation of the NAV echo, there may be a modest reduction in the total number of sections that can be acquired.
- This shows particular promise for correcting gross motion.
- This technique effectively corrects the images degraded by motion caused by long MR scans of a single position, pediatric examinations, etc.

- The mode of adaptive correction is entirely independent of other currently available techniques.
- This method could be combined with other artifact reduction techniques such as gradient moment nulling, ordered phase encoding or presaturation.

- ***Limitation***: it cannot correct for view-to-view z-axis displacement in conventional 2DFT transaxial images.
- However, it can correct for phase shifts due to z-axis intraview motion in images.

- There are interesting parallels and differences between the correction techniques for intraview motion described here and gradient moment nulling.
- Both techniques will correct phase shifts due to bulk motion of solid tissue but in contrast to gradient moment nulling, the adaptive technique ***specifically refocuses only the selected tissues***.

- This may permit the ***selective enhancement*** of specific structures in images on the basis of their unique motions while the detail of the surrounding tissues is suppressed.
- Offers interesting possibilities for quantitatively measuring or characterizing the physiologic motions of tissue structures with MR imaging.
- It may be thus suitable for removing the effects of respiratory motion unsharpness from MR angiograms, especially in the potential application of coronary artery imaging.

References

- Adaptive technique for High Definition MR Imaging of Moving Structures, Richard. L. Ehman, Joel. P. Felmlee, MR radiology, Oct'89.
- Correction of Motional Artifacts using Navigator echoes, R.J. Ordridge et all, MR Imaging, Volume 12, 1994.
- Motion tracking using navigator echoes, J.Tokuda et all, Academic Radiology, Jan 1994.
- Improved reduction of motion artifacts using navigator echoes, C.A. Clark et all, journal of Magnetic resonance, Sept 1999.